JOURNAL OF THE CANADIAN SOCIETY OF EXPLORATION GEOPHYSICISTS
VOL. 23, NO. 1 (DEC. 1987) P. 46-55

SEISMIC ATTENUATION AND POISSON'S RATIOS IN OIL SANDS FROM CROSSHOLE MEASUREMENTS[1]

COSTAS G. MACRIDES[2,3] AND ERNEST R. KANASEWICH[2]

ABSTRACT

Laboratory measurements of seismic attenuation are of interest but interpreting the results in terms of behavior at seismic frequencies can be problematic. In-situ measurements of attenuation in the Clearwater Formation near Cold Lake, Alberta, before and after steam stimulation, are presented here. These were extracted from data obtained during two well-to-well seismic tomography surveys initiated by Esso Resources Canada Limited.

The spectral ratio method as well as the concept of average frequency were used in order to measure attenuation before steam stimulating the formation. The values of Q_p obtained were close to 30 assuming a linear dependence of attenuation with frequency. By employing a modified spectral ratio technique and analyzing "before" and "after" seismic traces, a Q_p value close to 10 was found for the steam-invaded zone. The Poisson's ratio within the zone was calculated to be as high as 0.40. These findings indicate the presence of substantial amounts of viscous fluids introduced in the pore space by the process of steam injection. Furthermore, the increased attenuation within the heated zone is explained in terms of the dramatic increase of permeability within the zone as a result of bitumen mobilization. The field measurements were not optimized for determining attenuation or Poisson's ratios, so the results are significant in establishing that it is possible to obtain such parameters. Optimization of recording techniques will certainly allow one to obtain the spatial variation of these variables.

INTRODUCTION

Seismic attenuation properties of rocks can be investigated by laboratory studies (Toksöz *et al.*, 1979). Such studies employ frequencies in the kilo- and megahertz range in order to determine physical properties of very small samples, but interpreting these results in terms of behavior at seismic frequencies is problematic (Stewart *et al.*, 1984). The reason is that the mechanisms responsible for attenuation at ultrasonic frequencies may be entirely different from those in the seismic band. In addition, one would like to have information on the spatial variation of attenuation without having to obtain core samples. Therefore, of more interest are in-situ studies of seismic attenuation. It should not be forgotten that core samples are necessarily altered from their in-situ state. This sampling problem is particularly serious in oil sands due to their cohesionless character (Dusseault and Van Domselaar, 1982).

The purpose of this paper is to present Q values for oil sands calculated by a variety of techniques using well-to-well seismic measurements (Macrides *et al.*, 1985; Bregman *et al.*, 1986; Bregman, 1987). These measurements were initially taken as part of seismic tomography studies for the purposes of imaging the Clearwater Formation before and after steam injection (Macrides, 1987).

Geological description of the Clearwater Formation

The Clearwater Formation contains highly saturated oil sands and accounts for approximately one-half of the total bitumen in place at Cold Lake (Outtrim and Evans, 1977). The formation is gradational in thickness and ranges from 6 m in the south to over 60 m in the north. This reservoir, which occurs at depths of 410-450 m, has been the target of most pilot operations at Cold Lake to date. The Clearwater Formation has been interpreted as deltaic in origin (Outtrim and Evans, 1977). The Clearwater oil sands are only weakly cemented by the bitumen, and the reservoir body can be characterized as cohesionless. Oil gravity is 9-12° API (986 to 1007 kg/m^3), absolute permeability is 1 Darcy (1 μm^2),

[1]Presented at the C.S.E.G. National Convention, Calgary, Alberta, May 14, 1987. Manuscript received by the Editor April 22, 1987; revised manuscript received October 15, 1987.

[2]Department of Physics, The University of Alberta, Edmonton, Alberta T6G 2J1

[3]Present address: Department of Geological Sciences, The University of Manitoba, Winnipeg, Manitoba R3T 2N2

We would like to express our deep appreciation to Esso Resources Canada Limited for the Cold Lake seismic data in the well-to-well experiments and for their support in the form of grants and contracts. The efforts of Dr. Sube Bharatha, together with his technical and scientific expertise and advice, were greatly appreciated. The work was supported through a contract with the Alberta Oil Sands Technology and Research Authority (AOSTRA). Dr. Macrides would like to express his appreciation for an AOSTRA scholarship during this period as a Ph.D. graduate student. The DFS-V recording unit was obtained from capital grants from the Natural Sciences and Engineering Research Council of Canada (NSERC) and from AOSTRA.

oil viscosity in the reservoir is 100 000 cP (100 Pa.s), and porosity is 30%. Under reservoir conditions the oil, or bitumen, is immobile.

Bitumen saturation appears to be closely related to depositional environment and varies from 6% to 15% by weight. In contrast with the geologically older Athabasca oil sands, which consist almost entirely of quartz grains (and are characterized by higher degree of diagenesis and reduced porosity), the Clearwater sands contain, in addition to quartz, high percentages of feldspar, volcanic rock fragments and chert. For more detailed geological descriptions of the Cold Lake area and the Clearwater Formation the reader is referred to Harrison *et al.* (1981) and Putnam and Pedskalny (1983).

The Experiments

The data we employed in this study were collected from two well-to-well surveys. The first was a before and after steam injection seismic experiment conducted in the Cold Lake area in 1982. The second was a presteam seismic tomography experiment also in the Cold Lake area, executed in 1985. The target formation in both experiments was the Clearwater which had a thickness of 50 m at depths close to 450 m. The before and after survey made use of a single explosive source (Primacord) fired repeatedly at a fixed level within the one well for ten different depths of a single vertical-component receiver clamped within the other well. The sampling interval in the recording was 1 ms.

In the second experiment an airgun source at a pressure of 2300 PSI (16,000 kPa) was positioned at 24 different depths within the source well. Recording was through a DFS-V unit in the University of Alberta Mobile Seismic Laboratory from a downhole string of 24 hydrophones. The sampling interval was 0.5 ms. The spacing at sources and receivers was 3 m. A typical example of the recorded signals is shown in Figure 2. The horizontal distance, in both experiments, between source and receiver wells was close to 200 m.

Q measurements from the presteam tomography experiment

a) Using the spectral ratio method — Our procedure for measuring attenuation involved the spectral ratio method. This method has been applied successfully for measuring attenuation from vertical seismic profiles (Hauge, 1981). The technique requires the choice of a reference downhole pulse and the construction of spectral ratios between this and another downhole pulse.

Applying the same technique to our hole-to-hole seismic profiles can be more problematic. Due to the geometry of the experiment, see Figure 1, the range over which the various distances between source and receiver vary is limited. As a consequence, the success of the spectral ratio method will rely heavily on the good match between the frequency responses of the receivers. However, the use of a string of hydrophones receiving seismic pulses from a single shot is in favor of meeting this requirement.

Let us call x_0 the distance a seismic ray travels from source #1 to receiver #1, in Figure 1, and x the distance between the same source and receiver #24. The sonic logs, shown in Figure 3, indicate that there is no velocity contrast between the Clearwater Formation and the formation above it (Grand Rapids). Hence, no refraction of seismic rays is expected to occur at the interface. The amplitude of the seismic pulse at distance x_0 will be given by

$$A(x_0) = G(x_0)\, e^{\frac{-\pi f x_0}{v_P Q}} \qquad (1)$$

and the amplitude at distance x will be

$$A(x) = G(x)\, e^{\frac{-\pi f x}{v_P Q}} \qquad (2)$$

where f is frequency (in Hz), v_P is the phase velocity of the P-wave and Q is the quality factor of the medium characterizing its intrinsic attenuation. $G(x)$ is a frequency-independent function incorporating the effects of: 1) spherical divergence, 2) dependence of the pulse amplitude on impedance (Treitel and Robinson, 1966), 3) source strength and recorder gain, and 4) angular dependence of the radiation pattern, (Fehler and Pearson, 1984).

In order to construct spectral ratios between the two pulses we take the logarithm of the ratio of the two amplitudes at each frequency, choosing the pulse at x_0 as reference. Then:

$$\ln\left\{\frac{A(x_0)}{A(x)}\right\} = \ln\left\{\frac{G(x_0)}{G(x)}\right\} + \frac{(x-x_0)\pi f}{Q v_p} \qquad (3)$$

A plot of $\ln\{A(x_0)/A(x)\}$ versus frequency f will yield a linear graph from the slope of which the value of Q can be calculated. The implication is that Q and v_p are frequency independent. This can be a questionable assumption if a wide range of frequencies is considered but it is a useful first approximation for our purposes. The power spectral estimates for the two P-wave pulses and their spectral ratios plotted versus frequency are shown in Figure 4. It is worth mentioning that the P-wave spectra of seismograms 2 to 23 exhibited the same bimodal character as 1 and 24. From the slope (and its standard deviation) of the spectral ratio graph the value of Q was found to be equal to 27 ± 5. The various steps that were taken for reaching this result are summarized as follows:

1) A cosine bell taper window 80 points long (40 ms) was applied to the P-wave phases. The window was carefully applied as to avoid the high-frequency event which follows about 25 ms after the first arrival in record #1. Tapering is particularly essential for the study of individual phases in seismology in order to minimize

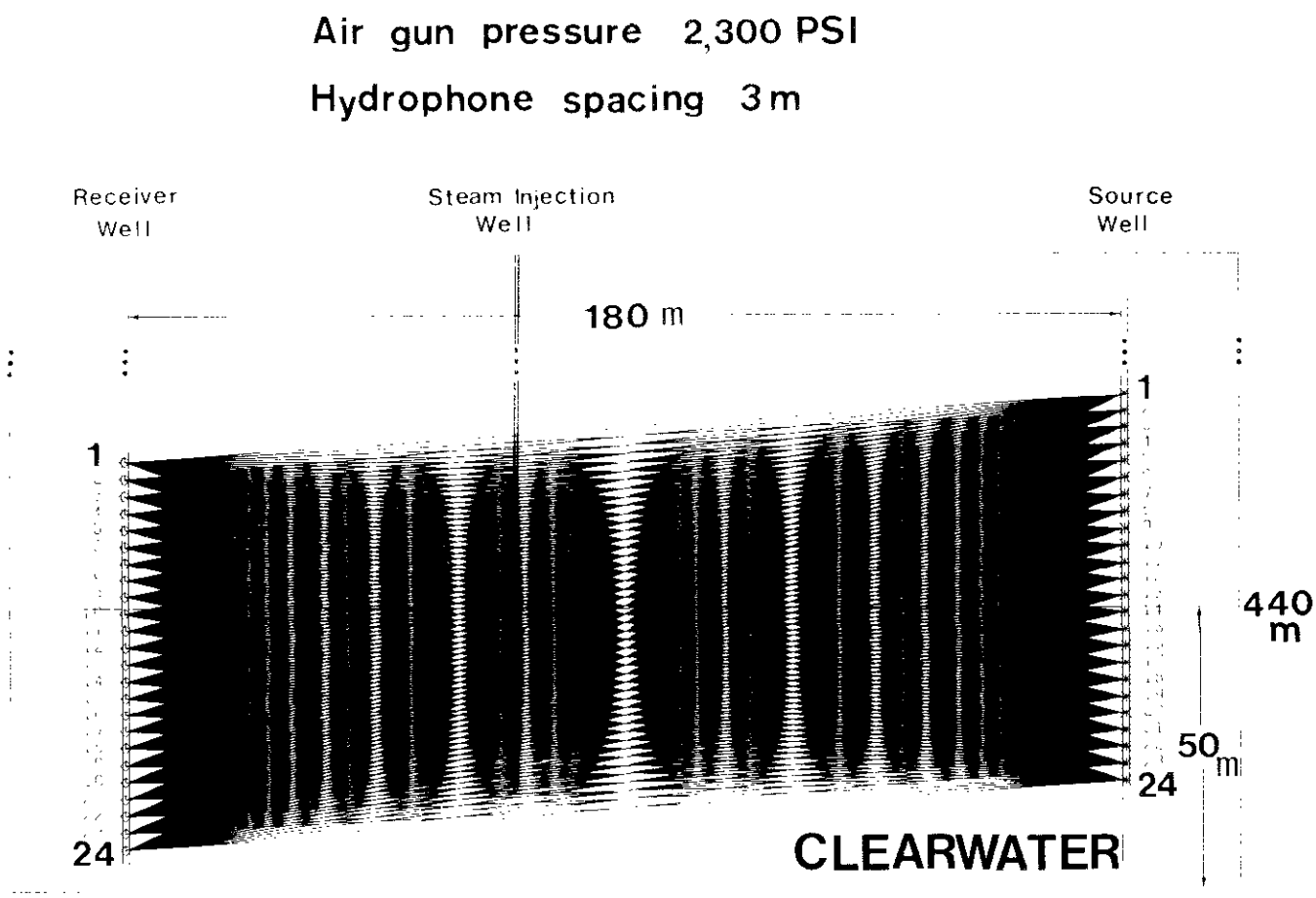

Fig. 1. Geometry of the presteam tomography experiment. The source well is separated from the receiver well by a distance of 180 m. Thickness of the Clearwater Formation is 50 m.

the effects of other phases and to avoid large discontinuities that may occur at the beginning and the end of the data vector (Kanasewich, 1981). Prior to this operation the low-frequency noise — up to 40 Hz — which was prominently present in the records was eliminated through band-pass filtering.

2) The data vector was padded with zeros until the total number of points in the time series was equal to $N' = 256 (= 2^8)$. The DC component of the time series was removed and the power spectrum was calculated using a fast Fourier transform and a Daniell (1946) window in the frequency domain. The result is given by

$$P(W) = \left\{ \frac{N'}{N(2m+1)} \right\} \sum_{W=0}^{N'/2} \{ F(W \quad j) F^*(W \quad j) \} \tag{4}$$

$$W \quad 0,1,2, \quad , N'/2$$

where $N = 80$, $N' = 256$ and m was chosen equal to 3. The star indicates a complex conjugate.

3) Statistical analysis of the spectral ratios was carried out in order to determine the probable error of the distribution. Then, any data points with residuals exceeding five times the probable error were discarded, (Margenau and Murphy, 1955). However, very few measurements qualified for such a rejection. Subsequently, the spectral ratio versus frequency graph was smoothed using a moving average window 7 points wide. Then a linear least-squares fit was applied to the data. A Q value of 27 ± 5 was obtained from the slope of the linear trend and equation (3). v_p was 2400 ± 40 m/s and was determined by the first arrival times.

At frequencies higher than 150 Hz the spectral ratios oscillate around the linear trend of the graph. This is probably caused by geological interference. For instance, although velocity contrast at the top of the Clearwater is zero, impedance contrast may not be zero. Hence, very low-amplitude reflections are possible from that interface interfering with the spectral estimates of the P-wave pulse arriving at receiver #1. Other interference is possible from a number of high-velocity carbonate stringers present in the Clearwater. These are clearly visible in the sonic logs. They are rather randomly distributed within the formation and are laterally discontinuous. They are very thin — about 2 m; hence, they will be visible only to the highest frequencies of the seismic energy. The fact that oscillations of the spectral ratios occur at high frequencies indicates that they are probably attributed to interference from these high-velocity stringers. If one does not want to include the oscillatory portion of the spectral ratios in the calculation of

Q, in which case the frequency range from 40 Hz to 150 Hz is considered, then the Q value obtained is 37 ± 7. It is of interest to mention that Schoenberger and Levin (1978) have tested and confirmed the effect of geological interference on spectral ratio calculations by constructing synthetic seismograms from sonic and density logs.

b) Using the concept of average frequency — Due to preferential absorption of higher frequencies, the shape of a travelling seismic pulse changes with distance from the source. Hauge (1981) has shown that the rate of change is dependent upon the attenuation according to the formula

$$\frac{d<f>_x}{dx} = -\left(\frac{2\pi}{Qv}\right)\left\{<f^2>_x - <f>_x^2\right\} \quad (5)$$

where $<f>_x$ is the average frequency of the pulse at distance x from the source. The quantity in the bracket in equation (5) is equivalent to the variance function $\sigma_x^2 = <(f-<f>_x)^2>_x$ which is always a positive number. Hence the rate of change of $<f>_x$ in equation (5) is always negative. In addition, at greater attenuation (smaller Q) the rate of change will be increased. Notice that the $<f>_x$ curve does not depend upon a reference depth. Furthermore, the $<f>_x$ curve makes use of information obtained from many channels, unlike the spectral ratio method which involves the analysis of only two pulses.

A plot of P-pulse average frequency versus shot-to-receiver distance — for source #1 of the experiment — is shown in Figure 5. The average frequency for each

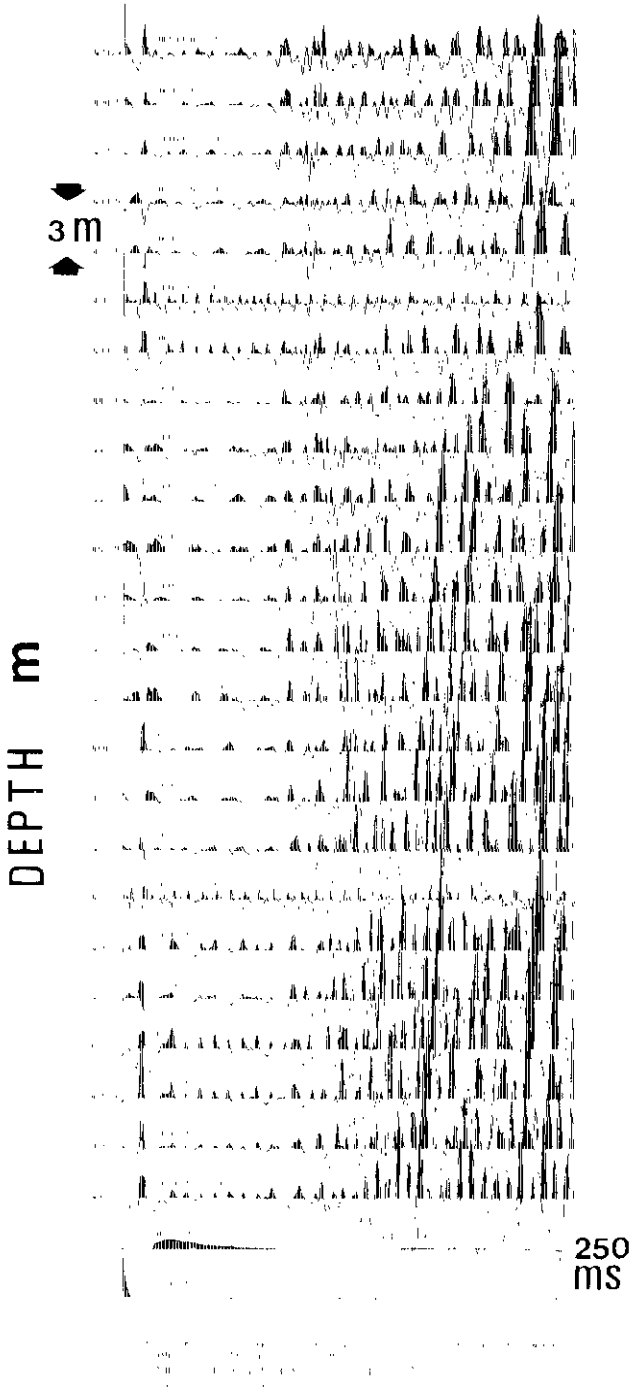

Fig. 2. Typical example of the recorded seismograms collected during the presteam tomography experiment using an airgun source and a string of hydrophone detectors. Data shown are for source at the uppermost location (#1).

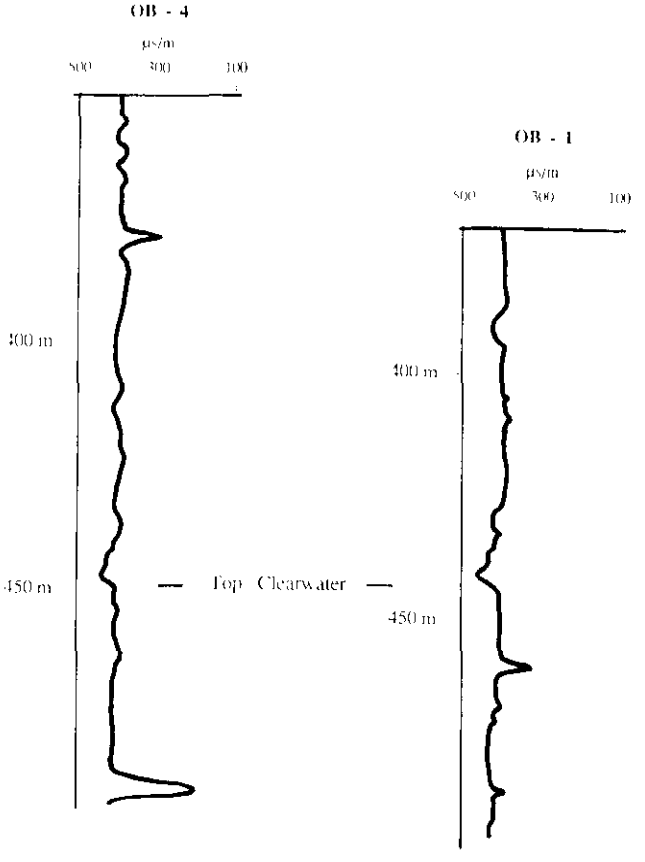

Fig. 3. Sonic logs for the source well (OB-1) and receiver well (OB-4) of the tomography experiment of Figure 1. Sonic log depths are with respect to Kelly Bushing (K.B.). K.B. elevation for OB-1 well was 626.2 m. K.B. elevation for OB-4 was 630.1 m. The two logs shown, redigitized at 1.5 m, have been aligned to take into account this difference in K.B. elevations.

pulse was calculated according to the definition given by Sheriff (1973):

$$\langle f \rangle_x = \frac{\sum f_i \{A_x(f_i)\}^2}{\sum \{A_x(f_i)\}^2} \quad (6)$$

where $\{A_x(f_i)\}^2$ is the power spectrum of the pulse at distance x from the source. The summation was carried over all the discrete frequencies f_i up to the Nyquist frequency.

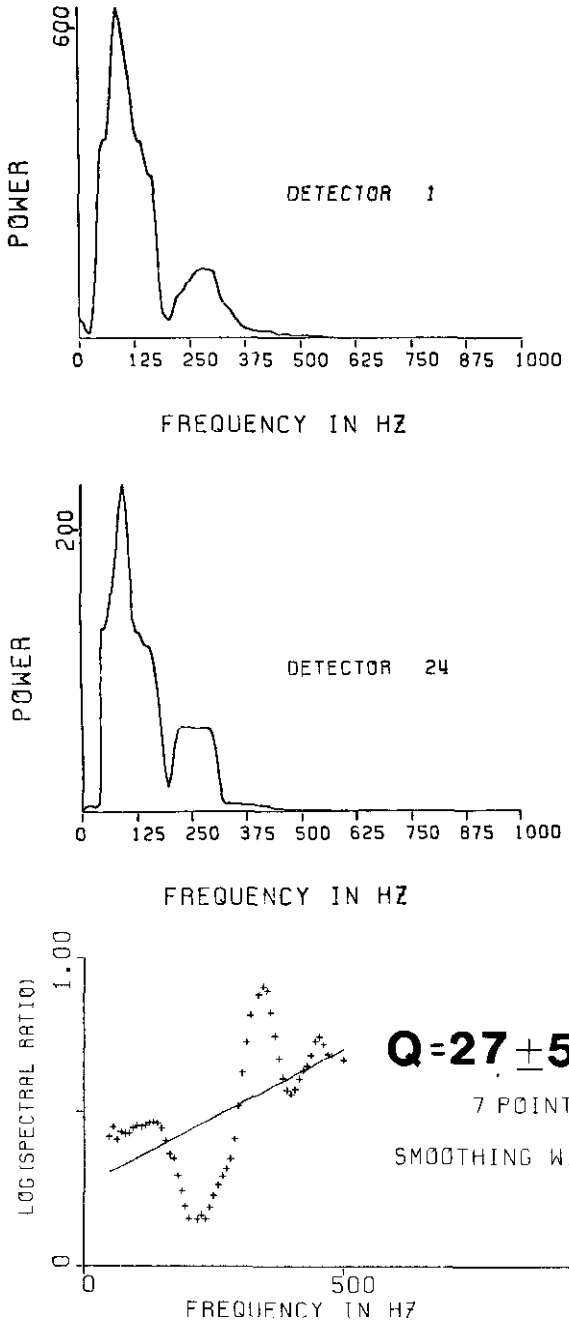

Fig. 4. Power spectra and spectral ratios of the P-wave pulses recorded at receivers #1 and #24 from source #1.

According to equation (5), $\langle f \rangle_x$ must be a monotonically decreasing function of the shot-to-receiver distance. Otherwise, negative values of Q will be encountered. From the slope of the function, the value of the attenuation can be calculated at each point of the graph. For the data shown in Figure 4, the closest curve to give a monotonic decrease of $\langle f \rangle_x$ is a straight line. This was calculated according to a least-squares fit. In this case $d\langle f \rangle_x/dx$ is a constant equal to the slope of the linear trend. Hence, σ_x^2 must also be a constant (provided Q is a constant) and was taken to be equal to the average variance of all the recorded pulses originating from source #1. Alternatively, one could let σ_x^2 be a variable, in which case a different Q value would be obtained from each point of the $\langle f \rangle_x$ versus x graph. Then, one can compute an average Q for the examined depth interval. However, Q is not expected to vary significantly within the depth range considered.

From the value of the slope $= -0.80$ (s m)$^{-1}$, the average variance $= 7300$ s^{-2}, and the P-wave velocity of 2400 m/s, a value of Q equal to 24 ± 8 was obtained. This is in satisfactory agreement with the value of Q which was obtained by the spectral ratio method (37 ± 7).

Calculation of Q Within the Steam-Invaded Zone

Our intention is to make use of the seismic data obtained from the before and after steam injection experiment shown in Figure 6. Analysis of the records — displayed in Figure 7 — has identified clear changes of the seismic signature after steam injection. There are changes in amplitudes and spectral characteristics, as well as time delays of the seismic pulses that have travelled through the steam zone. These results have formed the basis for suggesting that seismic tomography experiments could provide high resolution images of a steam-invaded zone, provided an adequately dense coverage of the target has been achieved (Macrides *et al.*, 1988). It is worth mentioning that the terminology "steam zone" is used to denote the zone of the seismic anomaly caused by steam injection and production. It

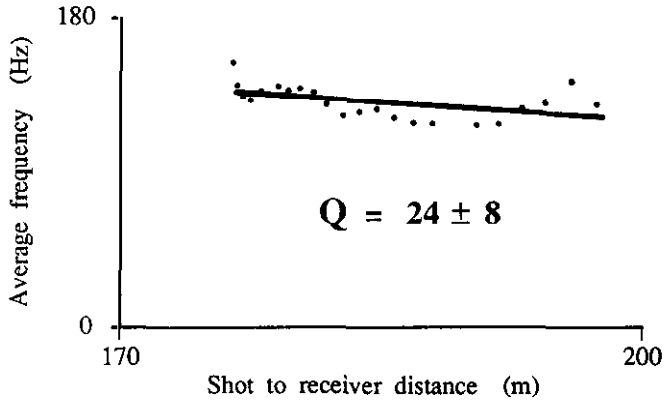

Fig. 5. Average downhole-pulse frequency versus shot-to-receiver distance for source #1 of the presteam tomography experiment.

should be noted that this zone will not necessarily coincide with a zone in which steam is present as vapor in the pore space.

Our purpose here is to show that a modified spectral ratio technique can be used in order to calculate values of seismic attenuation in the steam-invaded zone. Let us consider the raypath to receiver #1 of the before and after experiment of Figure 6. The before amplitude of the P-wave pulse will be given by

$$A_x(f) = G(x)\, e^{\frac{-\pi f x}{Q_p v_p}} \quad (7)$$

where x is the distance between source and receiver. $G(x)$ has the same meaning as in equation (1). Q_p is the intrinsic P-wave attenuation of the medium through which the seismic ray has travelled. In the poststeam environment the seismic ray will travel a certain distance Δx with attenuation Q_p' through the steam zone. Then the after amplitude of the pulse, assuming the total length of the raypath is still x, will be given by

$$A_x'(f) = G'(x)\, e^{\frac{-\pi f(x-\Delta x)}{Q_p v_p}}\, e^{\frac{-\pi f \Delta x}{Q_p' v_p'}} \quad (8)$$

Notice that $G'(x)$ will not necessarily be identical to $G(x)$, mainly because of the reflectivity at the boundary of the steam zone. Hence, the spectral ratio graph is expected to show a small positive intercept with the $\ln \{A_x(f)/A'_x(f)\}$ axis, after normalization of source strength and recorder gain has been performed. Taking the ratio of equations (7) and (8) and simplifying we obtain:

$$\ln\left\{\frac{A_x(f)}{A_x'(f)}\right\} = \ln\left\{\frac{G(x)}{G'(x)}\right\} + \pi\Delta x\left\{\left(\frac{1}{Q_p' v_p'}\right) - \left(\frac{1}{Q_p v_p}\right)\right\} f \quad (9)$$

where Q_p, v_p and Q_p', v_p' denote the values of seismic attenuation and velocity outside and inside the steam zone, respectively. Then, from a plot of $\ln\{A_x(f)/A_x'(f)\}$ versus f, the value of Q_p' could be calculated from the slope of the graph, provided the values of v_p, v_p', Δx and Q_p are known. v_p is 2400 m/s as determined from the first arrivals of the before traces. Q_p was found in the previous paragraphs to be close to 30.

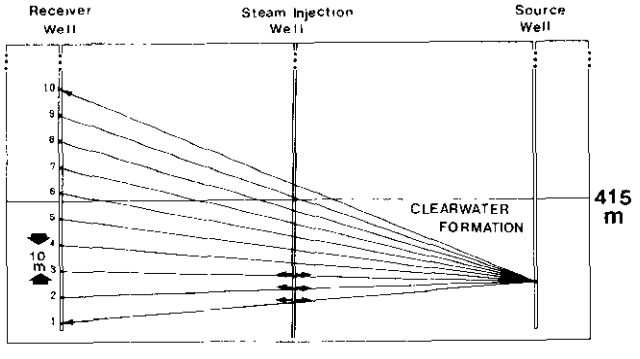

Fig. 6. Geometry of the before and after seismic experiment. The two wells were separated by a distance of 200 m. The horizontal arrows shown close to the bottom of the steam-injection well indicate the interval over which steam injection took place through the perforations. According to the sonic logs, the Clearwater Formation has the same velocity as the formation above it (Grand Rapids). Pressure during steam injection was close to 10 MPa.

A drop of 20% in the P-wave velocity is assumed to occur within the steam zone, hence, $v_p' = 2000$ m/s. This assumption is based on recent experimental results by Tosaya *et al.* (1984) who conducted an extensive laboratory study on a number of tar sands samples in order to determine the effect of elevated temperatures and varying bitumen content on seismic velocities. The results indicated that at high temperatures the magnitude of the drop in v_p appears to be qualitatively related to the decrease in oil viscosity with temperature. For instance, the drop in v_p for an Athabasca tar sand sample at 200° C was 70% compared to a base temperature of 20°, but for a tar sample with characteristics similar to Cold Lake conditions the drop was between 20% and 30%. It should be noted that viscosities of both the Athabasca and Cold Lake bitumen drop to about 10 cP (0.01 Pa.s) at 200° C but at initial reservoir conditions the viscosity of the Athabasca bitumen is about ten times greater.

From the observed P-phase delay of 1 ms at receiver #1 and from

$$\Delta T_p = \Delta x\left(\frac{1}{v_p'} - \frac{1}{v_p}\right) \quad (10)$$

Δx was found to be equal to about 12 m. A plot of logarithm of amplitude ratio of the before and after pulses at receiver #1 versus frequency is shown in Figure 8. Attenuation was calculated from

$$Q_p' = \frac{\pi\Delta x\, Q_p v_p}{(aQ_p v_p + \pi\Delta x)v_p'} \quad (11)$$

where a is the slope of the least-squares linear trend of the graph. Substitution of the known parameters in equation (11) gave $Q_p' = 7 \pm 2$. The frequency band considered was 30-240 Hz. For $v_p' = 1800$ m/s, Δ was 7.2 m and Q_p' was 5.5. We repeated the above calculations for the before and after seismic pulses arriving at receiver #2. In this case ΔT_p was 2 ms, hence $\Delta x = 24$ m. The plot of spectral ratios versus frequency is also shown in Figure 8. The frequency band considered was from 30 to 220 Hz. The calculation gave a value of Q_p' equal to 8 ± 2.

These low values of Q_p' suggest considerable amounts of attenuation of the seismic signals through the steam zone. This could be explained by the increased saturation of viscous fluids (mobilized heated bitumen) as well as less viscous ones (steam condensate) within the zone affected by the steam injection. It should be noted that the bitumen in the Clearwater is immobile under undisturbed reservoir conditions and from a hydrological point of view can be considered as part of the skeleton, because it reduces the permeability of the formation to

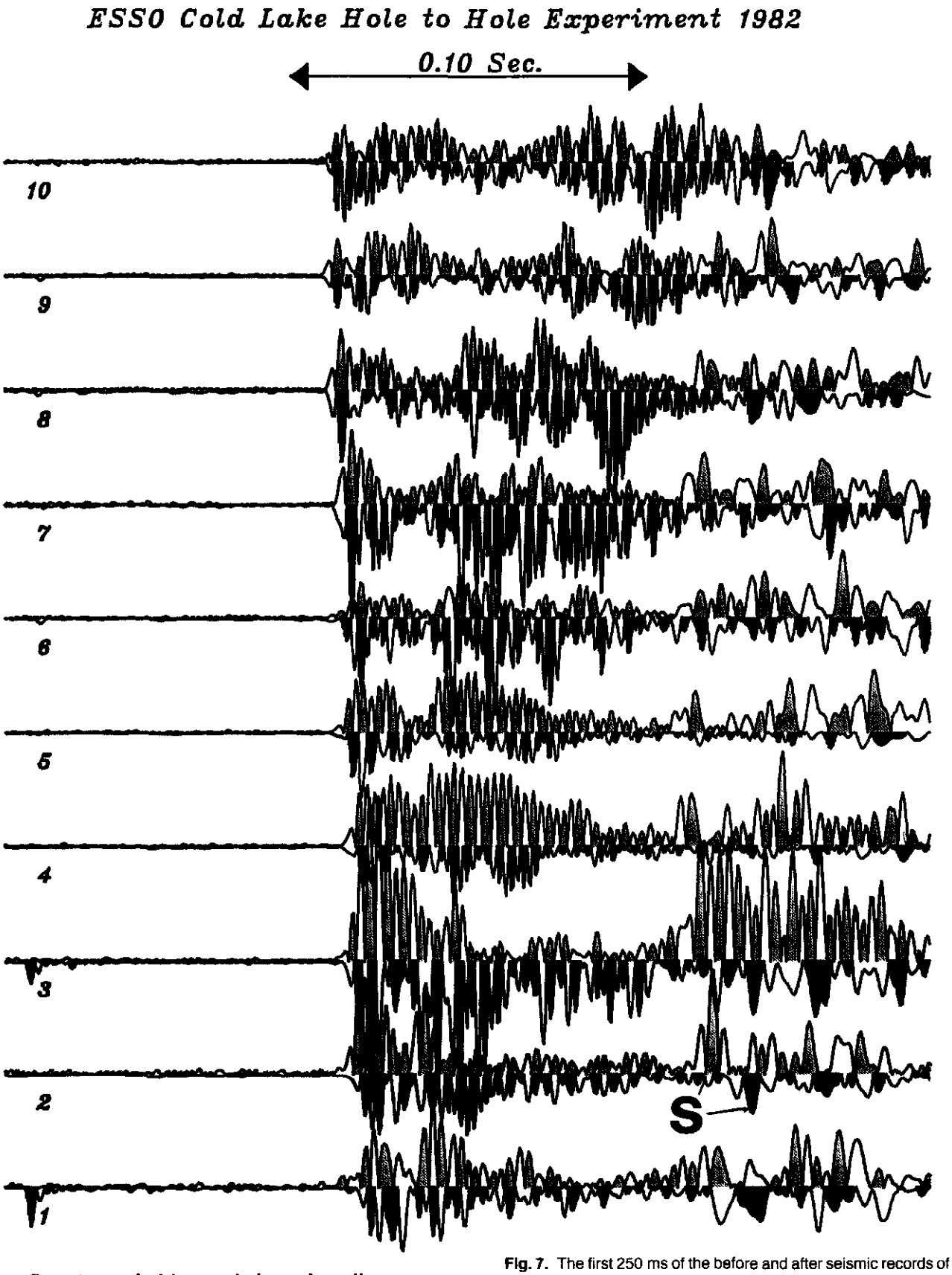

Fig. 7. The first 250 ms of the before and after seismic records of the experiment of Figure 6. The after records were obtained at the end of a 48-day steam-injection period. The seismic signals have been rectified in such a way as to allow plotting of the before records entirely above the zero-amplitude baseline and the after records entirely below it.

water by a factor of at least 100 with respect to the permeability of clean sands similar to the McMurray Formation (Harris and Sobkowicz, 1977).

Normally, since attenuation Q^{-1} is proportional to viscosity (Nyland, 1985) one should expect a drop in attenuation at higher temperatures. However, at elevated temperatures bitumen is able to flow with the result that permeability increases dramatically. This could possibly explain our observed low Q values in the heated zone. Attenuation has been found to increase with permeability (Nur *et al.*, 1980) in agreement with the notion that local flow is responsible for wave attenuation (O'Connell and Budiansky, 1977). In addition, the increased microcrack porosity created in the heated zone by the injection of highly pressurized steam is expected to further contribute to an increase of attenuation in the anomalous zone.

Notice, in Figure 8, that in the frequency range of 140-200 Hz, the spectral ratios indicate a linear regression trend with greater slope, hence, lower Q and higher attenuation. This might come in support of recent theoretical and experimental results showing evidence of an absorption peak at high frequencies beyond which attenuation decreases (Winkler and Nur, 1982; Jones and Nur, 1983). This peak is theoretically predicted for a single relaxation time or a very narrow distribution of relaxation times. According to results reported by Jones (1986), this absorption peak is expected to occur, for a tar sand material at a temperature of 200° C, at frequencies close to 300 Hz. At normal reservoir temperatures

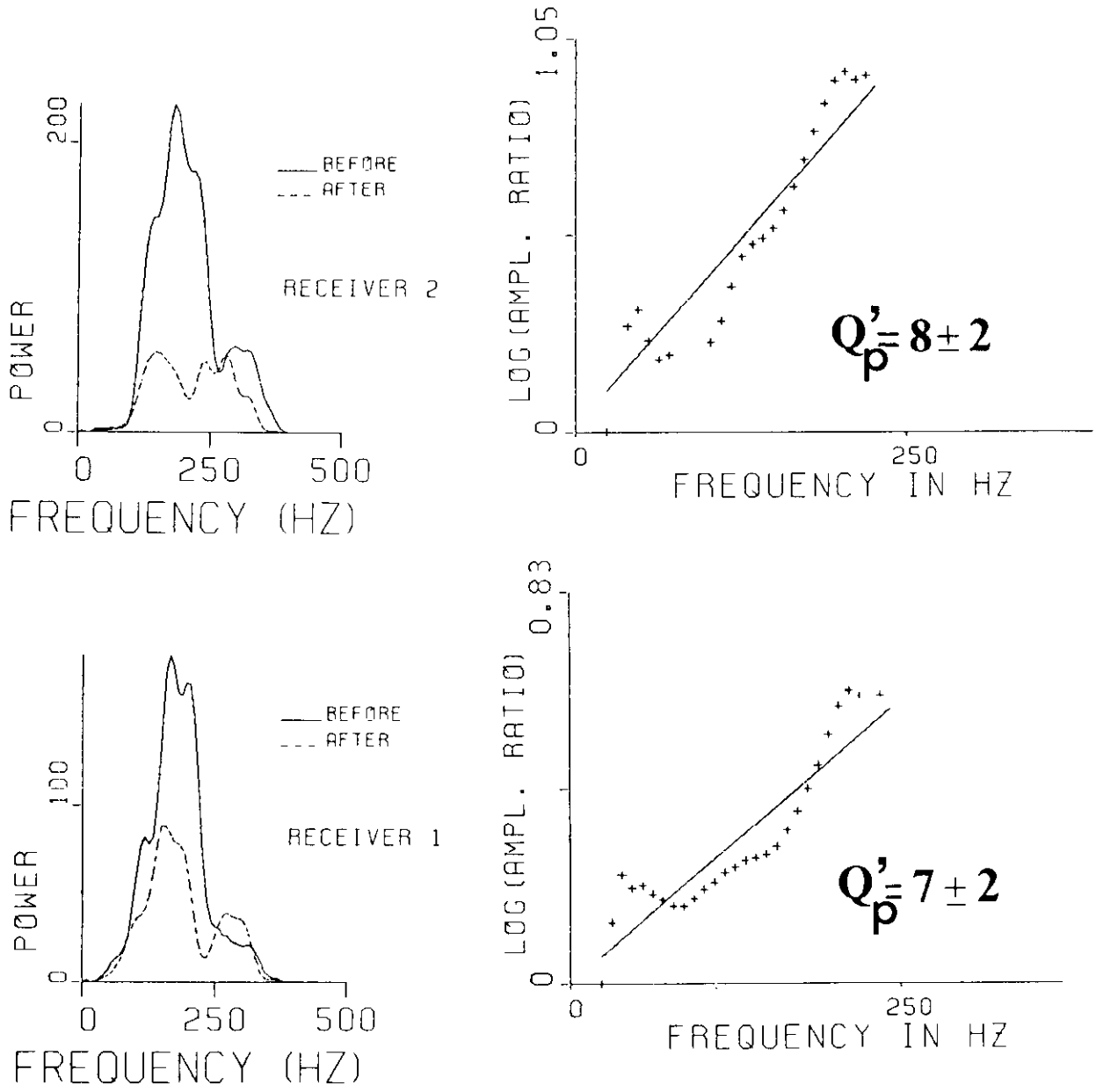

Fig. 8. Before and after power spectra of the P-pulses at receivers #1, #2, and their spectral ratios plotted versus frequency. The Q' values were calculated according to the linear regression results and equation (11) in the text.

the characteristic frequency is shifted towards much lower values (around 3 Hz).

Additional evidence of increased fluid saturation in the heated zone was provided by the following calculation. Clear before and after S-wave pulses have been observed (Figure 7) in the records of receiver #2, in addition to the P-waves. The S-wave pattern is highly complex because of the large delays introduced by the large relative velocity decrease after steam injection. Trace 6 shows the S-wave unmodified on rays not passing through the steam zone and not obscured by a P-SV reflection as on traces 7 to 10. Traces 1 to 3 show the S-wave with large delays and lower frequency in the after steam seismograms. While P-wave delay after injection was 2 ms in these records, the delay for the S-pulse was 10 ms. From these time delays, a known Poisson's ratio $\sigma = 0.30$ (from laboratory measurements on core samples; S. Bharatha, Esso Resources, *pers. comm.*) in the undisturbed formation, equation (10),

$$\Delta T_s = \Delta x\left(\frac{1}{v_s'} - \frac{1}{v_s}\right) \quad (12)$$

and

$$\frac{v_s'^2}{v_p'^2} = \frac{0.5 - \sigma'}{1 - \sigma'} \quad (13)$$

the Poisson's ratio σ' within the steam-invaded zone was found to be as high as 0.40. It may appear at first sight that the logic behind this calculation is circular. Equations (10) and (12), from which v_s' is derived, form a system of two equations with three unknowns: v_s', v_p', and Δx. Therefore, one has to start with an assumption for v_p'. For v_p' 20% less than v_p we found $\sigma' = 0.40$. For lower values of v_p', σ' increases. For example, for v_p' 30% less than v_p, σ' was 0.42. Hence, our calculations are weakly dependent on the choice of v_p' and consistently lead to high Poisson's ratios within the zone of interest. Poisson's ratio is an excellent indicator of the presence or absence of steam within a porous medium. This statement is supported by experimental studies (Domenico, 1974; Nur *et al.*, 1980). There is good evidence of Poisson's ratios as low as 0.12 in steam-dominated geothermal fields (Majer and McEvilly, 1979). The high Poisson's ratios we have identified in our steam-invaded zone indicates that the zone is dominated by steam condensate rather than steam. This is not surprising in view of the relatively small injection period (48 days) and the fact that the seismic measurements were taken during the first cycle of the steam stimulation program.

Finally, we carried out spectral analysis of the before and after S-wave pulses at receiver #2 in order to calculate S-wave attenuation within the steam zone. We employed the technique we discussed earlier for calculating Q_p'. For the S case, v_p, Q_p and v_p' in equation (11) should be replaced by v_s, Q_s and v_s'. Hence:

$$Q_s' = \frac{\pi \Delta x\, Q_s v_s}{(aQ_s v_s + \pi \Delta x) v_s'} \quad (14)$$

v_s was calculated from the presteam Poisson's ratio to be 1200 m/s and v_s' was found from equations (10) and (12) to be 800 m/s for $v_p' = 2000$ m/s.

Q_s could not be determined from our seismic experiments: direct S-arrivals were not recorded in the presteam tomography experiment and were severely disturbed by reflections from reflectors below the Clearwater in records #7 to #10 of the before and after experiment. However, we found that the calculation of Q_s' is only weakly dependent on Q_s in equation (14). For $Q_s = 60$ we found $Q_s' = 10.4$, while for $Q_s = 30$, Q_s' was 9.5. For $v_p' = 1800$ m/s, we obtained $Q_s = 8.3$ and 7.6 respectively. These values of Q_s' are close to the values we obtained for Q_p'. This may be another indicator of high fluid saturation within the steam zone. Murphy (1982) has provided experimental evidence that Q_p is roughly equal to $0.5Q_s$ for fluid saturations less than 90% (in agreement with the theoretical results of Mavko and Nur, 1979) and that Q_p is approaching Q_s at higher saturations. The spectra of the before and after S-pulses at receiver #2, as well as their spectral ratios, plotted versus frequency, are shown in Figure 9.

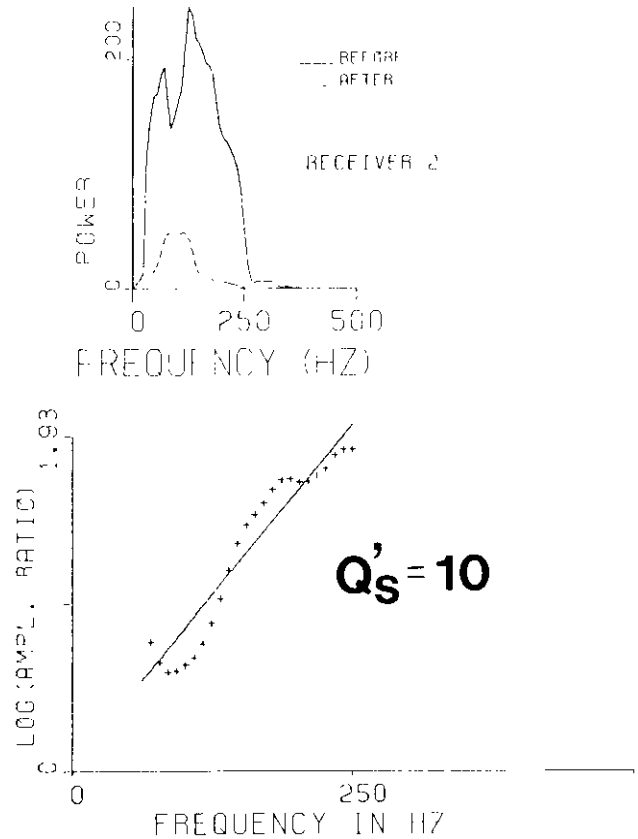

Fig. 9. Before and after power spectra of the S-pulses at receiver #2 and their spectral ratios plotted versus frequency. Notice the shift of the spectra towards lower frequencies, compared to the spectra of the P-waves of Figure 7.

CONCLUSION

Well-to-well seismic data were used to determine the in-situ attenuation of the Clearwater Formation before and after steam injection.

A variety of techniques were used involving the spectral ratio method and the concept of average frequency of a seismic pulse. It was found that Q_p in the presteam environment is close to 30. Considerably higher values of attenuation were found within the steam zone. These are attributed to large amounts of viscous dissipation of the seismic energy in the fluids introduced within the pore space during the steam injection operation. In addition there seems to be some evidence of a frequency dependence of Q, attenuation being greater in the frequency band of 140-200 Hz. Normally, one should expect higher Q at higher temperatures. The observed low Q values in the heated zone were explained in terms of the dramatic increase of permeability in the zone due to bitumen mobilization. If this is true, then it is entirely possible that one could use an accurate mapping of Q for the purposes of making in-situ measurements of permeability during enhanced heavy oil recovery operations.

By exploiting before and after P- and S-wave traveltimes, it was possible to obtain an estimate of Poisson's ratio within the steam zone. This was found to be quite high, indicating the presence of large amounts of steam condensate within the zone.

REFERENCES

Bregman, N.D., 1987, Tomographic inversion of crosshole seismic data: Ph.D. thesis, Univ. of Toronto.

———, Chapman, C.H. and Bailey, R.C., 1986, Cross-hole tomography using ray tracing: Presented at the 56th Ann. Internat. Mtg., Soc. Explor. Geophys., Houston, paper 513.7.

Daniell, P.J., 1946, Discussion on symposium on autocorrelation in time series: Supp. J. Roy. Stat. Soc. **8**, 88-90.

Domenico, S.N., 1974. Effect of water saturation on seismic reflectivity of sand reservoirs encased in shale: Geophysics **39**, 759-769.

Dusseault, M.B. and Van Domselaar, H.R., 1982, Unconsolidated sand sampling in Canadian and Venezuelan oil sands: 2nd UNITAR conference on the future of heavy crudes and tar sands, 336-348.

Fehler, M. and Pearson, C., 1984, Cross-hole seismic surveys: Applications for studying subsurface fracture systems at a hot dry rock geothermal site: Geophysics **49**, 37-45.

Harris, M.C. and Sobkowicz, J.C., 1977, Engineering behaviour of oil sand, *in* Redford, D.A. and Winestock, A.G., Eds., The oil sands of Canada-Venezuela: Can. Inst. Min. Metallurg. Special Vol. **17**, 270-281.

Harrison, D.B., Glaister, R.P. and Nelson, H.W., 1981, Reservoir description of the Clearwater oil sand, Cold Lake, Alberta, Canada, *in* The future of heavy crude and tar sands: McGraw-Hill Inc., 264-279.

Hauge, P.S., 1981, Measurements of attenuation from vertical seismic profiles: Geophysics **46**, 1548-1558.

Jones, T.D., 1986, Pore fluids and frequency-dependent wave propagation: Geophysics **51**, 1939-1953.

——— and Nur, A., 1983, Velocity and attenuation in sandstone at elevated temperatures and pressures: Geophys. Res. Lett. **10**, 140-143.

Kanasewich, E.R., 1981, Time sequence analysis in geophysics: 3rd ed., Univ. of Alberta Press.

Macrides, C.G., 1987, Seismic tomography in oil sands for monitoring thermal recovery processes: Ph.D. thesis, Univ. of Alberta.

———, Kanasewich, E.R. and Bharatha, S., 1985, Cross-borehole seismic imaging in steam injection projects: Presented at the 1985 Nat. Conv., Can. Soc. Expl. Geophys./ Can. Geophys. Union, Calgary, paper VV-5.

———, ———, ———, 1988, Multiborehole seismic imaging in steam injection heavy oil recovery projects: Geophysics, in press.

Majer, E.L. and McEvilly, T.V., 1979, Seismological investigations at the Geysers geothermal field: Geophysics **44**, 246-269.

Margenau, H. and Murphy, G.M., 1955, The mathematics of physics and chemistry: D. Van Nostrand Co.

Mavko, G.M. and Nur, A., 1979, Wave attenuation in partially saturated rocks: Geophysics **44**, 161-178.

Murphy III, W.F., 1982, Effects of partial water saturation on attenuation in Massillon sandstone and Vycor porous glass: J. Acoust. Soc. Am. **71**, 1458-1468.

Nur, A.M., Walls, J.D., Winkler K. and DeVilbiss, J., 1980, Effects of fluid saturation on waves in porous rocks and relations to hydraulic permeability: J. Soc. Petr. Eng. **20**, 450-458.

Nyland, E., 1985, Seismic attenuation in oil sand: AOSTRA J. Res. **2**, 47-51.

O'Connell, R.J. and Budiansky, B., 1977, Viscoelastic properties of fluid-saturated cracked solids: J. Geophys. Res. **82**, 5719-5735.

Outtrim, C.P. and Evans, R.G., 1977, Alberta's oil sands reserves and their evaluation, *in* Redford, D.A. and Winestock, A.G., Eds., The oil sands of Canada-Venezuela: Can. Inst. Min. Metallurg. Special Vol. **17**, 36-66.

Putnam, P.E. and Pedskalny, M.A., 1983, Provenance of Clearwater Formation reservoir sandstones: Bull. Can. Petr. Geol. **31**, 148-160.

Schoenberger, M. and Levin, F.K., 1978, Apparent attenuation due to intrabed multiples, II: Geophysics **43**, 730-737.

Sheriff, R.E., 1973, Encyclopedic dictionary of exploration geophysics: Soc. Expl. Geophys.

Stewart, R.R., Huddleston, P.D. and Kan, T.K., 1984, Seismic versus sonic velocities: a vertical seismic profiling study: Geophysics **49**, 1153-1168.

Toksöz, M.N., Johnston, D.H. and Timur A., 1979, Attenuation of seismic waves in dry and saturated rocks: I. Laboratory measurements: Geophysics **44**, 681-690.

Tosaya, C.A., Nur, A.M. and Da Prat, G., 1984, Monitoring of Thermal EOR Fronts by seismic methods: Soc. Petr. Eng., Tech. Paper SPE-12744, 6 pp.

Treitel, S. and Robinson, E.A., 1966, Seismic wave propagation in layered media in terms of communication theory: Geophysics **31**, 17-32.

Winkler, K.W. and Nur, A., 1982, Seismic attenuation: effects of pore fluids and frictional sliding: Geophysics **47**, 1-15.